Multi Detection Joint Integrated Probabilistic Data Association Using Random Matrices with Applications to Radar-Based Multi Object Tracking

MICHAEL SCHUSTER
JOHANNES REUTER
GERD WANIELIK

In extended object tracking, a target is capable to generate more than one measurement per scan. Assuming the target being of elliptical shape and given a point cloud of measurements, the Random Matrix Framework can be applied to concurrently estimate the target's dynamic state and extension. If the point cloud contains also clutter measurements or origins from more than one target, the data association problem has to be solved as well. However, the well-known joint probabilistic data association method assumes that a target can generate at most one detection. In this article, this constraint is relaxed, and a multi-detection version of the joint integrated probabilistic data association is proposed. The data association method is then combined with the Random Matrix framework to track targets with elliptical shape. The final filter is evaluated in the context of tracking smaller vessels using a high resolution radar sensor. The performance of the filter is shown in simulation and in several experiments.

Manuscript received October 31, 2015; revised May 31, 2016; released for publication October 17, 2016.

Refereeing of this contribution was handled by Karl Granstrom.

Authors' addresses: M. Schuster and J. Reuter, Institute of System Dynamics, Konstanz University of Applied Sciences (E-mail: michael.schuster,johannes.reuter@htwg-konstanz.de). G. Wanielik, Professorship of Communication Engineering, Chemnitz University of Technology (E-mail: gerd.wanielik@etit.tu-chemnitz.de).

1557-6418/17/$17.00

I. INTRODUCTION

Radar systems have become standard for many automotive applications like adaptive cruise control or lane change assistance. Customarily, these sensors have the advantage that they need low mounting space, have low power consumption, are available at low cost, and still have a good resolution for ranges up to approx. 200 m. These features make the sensor also interesting for alternative applications. In this paper, these kind of radar sensors are considered for application in marine environment. Radars in this context typically operate with 3 GHz or 9 GHz and, as a consequence, have rather large apertures and high energy consumption. Small unmanned surface vessels (USV) usually do not have sufficient space or energy resources for such systems. On the other hand, very often these types of vessels operate in harbors or on rivers and in general require only short range surveillance [1]. Thus, automotive radar sensors (ARS) are an interesting alternative.

When applying these sensors in marine environment, the extension of a scanned vessel in comparison to sensor resolution is very high. Hence, at each scan, a point cloud of detections from an object is provided by the sensor. This leads to an extended target tracking problem. In order to solve this, numerous algorithms have already been proposed, see e.g. the surveys in [2] and [3].

Assuming the sensor does not generate stable but fast fluctuating reflection centers, an estimation of the target extent can be obtained by analyzing the noise distribution. If the measurements are randomly distributed over the target extent, or the noise of the measurements is correlated with the target's size, [4] presented an approach for simultaneously estimating the state and extension of a target. There, the target's physical extension is assumed to be of an elliptical shape and is represented by a symmetric positive definite random matrix. For many real sensors, the measurement spread is only partially dependent on the target's extent and also on the sensor's accuracy. Thus, [5] made the proposition to model this spread as a linear combination of extension noise and measurement noise. Due to the heuristics in [5], [6] derived a more complex filter update step which improves the estimation results. A unification of [4] and [5] was proposed in [7] and further extended for non-elliptical models in [8]. An alternative for arbitrary shapes is presented in [9], where Random Hypersurface Models are used to estimate the extent of an object.

Besides the pure state estimation task, the measurement to track data association problem has to be solved. A typical problem in Extended Target Multi Object Tracking (ET-MOT) is shown in Figure 1. Each object generates several detections, and, in combination with the clutter measurements, using the detections only it is unclear which target created how many detections, and where these measurements are located. A first data association method in the context of the Random Matrix

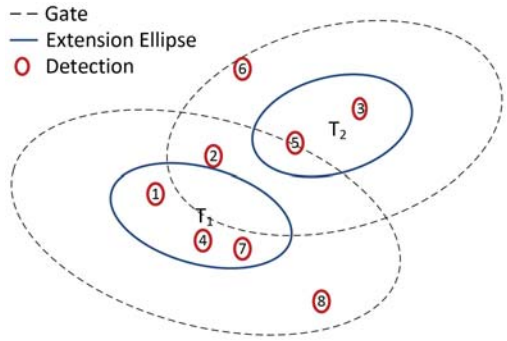

Fig. 1. Typical situation in extended object tracking if the targets have an elliptical shape. The dashed lines indicate a typical association threshold. Only detections within are considered for update of the central track.

framework is given in [10] and [11], where the Probabilistic Multi-Hypothesis algorithm is applied. Using Random Finite Sets, various Multi Object trackers have been presented, e.g. in [12]–[14]. Although the results of the Labeled Multi Bernoulli in [14] are very promising, in the authors opinion it is worth to also take a look at more traditional approaches and to investigate how these can be modified to be applied in ET-MOT.

One of the most popular methods for assigning measurements to a track is the Probabilistic Data Association (PDA) filter [15]. It performs a measurement update for each possible association and computes for each association the corresponding likelihood that the selected measurement is correct, i.e. was originated by the target. The a posteriori estimate of the track is then given by the weighted sum of the updated state estimates. In case that more than one object is present, the PDA is extended to the Joint PDA (JPDA), which also reflects the partitioning of the measurements to the tracks when calculating the association likelihood.

Besides the state estimate, for a multi-object tracker, the existence probability is of relevance, as well. Therefore, [16] modified the PDA to integrate also the estimation of the existence likelihood into the filtering and data association process. The new methods are named IPDA for the single object case and JIPDA for the multi-object case [17], respectively, where the letter 'I' stands for "Integrated."

All these PDA algorithms rely on the common assumption that an object can generate at most one measurement during a sensor scan cycle. As already stated in the abstract, for extended object tracking, this assumption does not hold in general. To make PDA feasible in this context, spatial clustering of the detections in combination with a JPDA is proposed in [18]. A version of the PDA that can handle more than one detection was presented in [19] and a Multi-Detection JPDA in [20]. The MD-JPDA was used to handle multi-path reflections from over-the-horizon radars. With the Generalized PDA, also the existence estimation was introduced into the MD-PDA by [21]. Since for multi-target tracking algorithms, the existence likelihood estimation is essential, in this paper, a Multi-Detection JIPDA (MD-JIPDA) is derived, as an extension to the JIPDA to assign more than one measurement to an object.

The structure of this paper is as follows: First, the general derivation of the MD-JIPDA is given in section II. In section III, an implementation of the MD-JIPDA that uses the concept of Random Matrices is proposed. It gives a short introduction to Random Matrices and also illustrates an approximation scheme of the MD-JIPDA to make it real-time applicable. Some results of Monte Carlo Simulations for different sensor characteristics and scenarios are shown in section IV. In the context of tracking smaller vessels in close distance using an automotive radar sensor on USV, also some experimental results are presented in section V, and conclusions are drawn in section VI.

II. MULTI DETECTION–JOINT INTEGRATED PROBABILISTIC DATA ASSOCIATION

In the original Integrated Probabilistic Data Association (IPDA) approach, a track is considered to consist of two components [22, p. 142]: The object's dynamic states and the object's existence estimates. While the dynamic state is a continuous random variable, the existence is a binary variable that only can take the values "object exists" and "object does not exist." One central assumption of the IPDA filter, as proposed in [16], is that an object can generate at most one measurement at time k. The Generalized Probabilistic Data Association Filter relaxes this constraint in such a way that up to $n_{\max}$ measurements can be originated by a single object. The obtained GPDA filter can be applied for multi-object cases only if the objects are well separated in the measurement space. If the targets are in close proximity to each other, the GPDA will tend to merge tracks. To avoid this, in this section, a new algorithm, that can be used to consider joint track to measurement associations is described.

In the following, the dynamic state of track t at time k will be referred to as $\mathbf{x}_k^t$, and χ_k^t describes the event that the object exists and $\bar{\chi}_k^t$ the complementary event. If a set of new measurements is received, for each track, only those measurements are considered that fall into some elliptical association gate with constant probability P_G. Tracks that share at least one common measurement in their association gate are put together in a new association cluster, and a joint cluster volume V_k can be computed. Since gating and track clustering are commonly known techniques, the reader is referred to the literature for further information, e.g. [23, p. 334ff]. The set of n_k gated measurements will be denoted as $\mathbf{Z}_k = \{\mathbf{z}_k^1, \ldots, \mathbf{z}_k^{n_k}\}$ and $\mathbf{Z}^k$ the measurements received up to time k.

From the Bayes' filter update equation, the posterior probability of the target existence is given by:

$$p(\chi_k \mid \mathbf{Z}^k) = \frac{p(\mathbf{Z}_k \mid \chi_k^t)p(\chi_k \mid \mathbf{Z}^{k-1})}{p(\mathbf{Z}_k \mid \bar{\chi}_k^t)p(\bar{\chi}_k^t \mid \mathbf{Z}^{k-1}) + p(\mathbf{Z}_k^t \mid \chi_k)p(\chi_k^t \mid \mathbf{Z}^{k-1})} \tag{1}$$

The predicted existence probability from time $k-1$ is computed from

$$p(\chi_k^t \mid \mathbf{Z}^{k-1}) = p_{\text{surv}} \cdot p(\chi_k^t \mid \mathbf{Z}^{k-1}), \tag{2}$$

where, for simplicity, the probability of object survival p_{surv} is here considered as state independent. Using a proper existence time constant τ_χ for a track, the probability of survival is only conditioned on the sample time T with

$$p_{\text{surv}} = e^{-T/\tau_\chi}. \tag{3}$$

To evaluate the likelihoods in (1), the following assumptions are made:

- Clutter is uniformly distributed over the volume V:

$$p_s^{Cl}(n) = V^{-n}$$

- The number of clutter measurements is Poisson distributed with constant clutter rate λ:

$$p_c^{Cl}(n) = \frac{(\lambda V)^n}{n!} e^{-\lambda V}$$

- An object is detected by the sensor with probability P_D.
- The number of measurements m generated by one object t follows an arbitrary distribution $p_c^t(m)$.
- The spatial model for a single measurement of an object t is denoted $p_s^t(\mathbf{z}_k \mid \mathbf{x}_k)$, which is typically a Gaussian of the form

$$p_s^t(\mathbf{z}_k \mid \mathbf{x}_k^t) = \frac{1}{P_G}\mathcal{N}(\mathbf{z}_k; \mathbf{H}\mathbf{x}_k, \mathbf{\Sigma}_k),$$

where $\mathbf{H}$ is the observation matrix and $\mathbf{\Sigma}_k$ the corresponding covariance.

A. Joint Association Probability

Let $\mathcal{H}_{i,j}$ denote a joint association event that describes one hypothesis how the n_k measurements within an association cluster have been created. The joint association events can be grouped into joint detection events $\mathcal{D}_i$ which assign the same detection count pattern. One pattern assigns a specific measurement count m_t to track t, e.g. for the situation in Figure 1 the event $\mathcal{H}_{i,1} = \{\{4,7\},\{3,5,6\}\}$ that assigns measurements $M4$ and $M7$ to track one, and $M3, M5, M6$ to track two belong to the same detection event $\mathcal{D}_i$ as $\mathcal{H}_{i,2} = \{\{1,7\},\{3,5,6\}\}$.

The a posterior probability of a joint event $\mathcal{H}_{i,j}$ is defined as

$$\begin{aligned} p(\mathcal{H}_{i,j} \mid \mathbf{Z}^k) &= \eta_{\mathcal{H}} \cdot p(\mathbf{Z}_k, n_k, \mathcal{H}_{i,j}, \mathcal{D}_i \mid \mathbf{Z}^{k-1}) \\ &= \eta_{\mathcal{H}} \cdot p(\mathbf{Z}_k \mid n_k, \mathcal{H}_{i,j}, \mathcal{D}_i, \mathbf{Z}^{k-1}) \\ &\quad \times p(n_k \mid \mathcal{H}_{i,j}, \mathcal{D}_i, \mathbf{Z}^{k-1}) \\ &\quad \times p(\mathcal{H}_{i,j} \mid \mathcal{D}_i, \mathbf{Z}^{k-1}) \cdot p(\mathcal{D}_i \mid \mathbf{Z}^{k-1}). \end{aligned} \tag{4}$$

With this definition, in order to compute the individual probabilities for each joint detection event, the tracks can be separated in two sets:

1) $\mathcal{T}_{\text{mis}}(\mathcal{D}_i)$: Set of tracks with no allocated measurements
2) $\mathcal{T}_{\text{hit}}(\mathcal{D}_i)$: Set of tracks with at least one allocated measurement

Let further $\mathcal{A}_{\text{mis}}^t$ denote an event, where no measurement is assigned to track t and $\mathcal{A}_{\text{hit}}^t$ for at least one assigned detection.

For each track t in $\mathcal{T}_{\text{mis}}(\mathcal{D}_i)$ the prior probability is

$$p(\mathcal{A}_{\text{mis}}^t \mid \mathbf{Z}^{k-1}) = 1 - P_D^t P_G^t p(\chi_k^t \mid \mathbf{Z}^{k-1}),$$

and if one or more measurements are assigned

$$p(\mathcal{A}_{\text{hit}}^t \mid \mathbf{Z}^{k-1}) = P_D^t P_G^t p(\chi_k^t \mid \mathbf{Z}^{k-1}).$$

With these two definitions, the prior probability of a joint detection event is [22, p. 161]

$$\begin{aligned} p(\mathcal{D}_i \mid \mathbf{Z}^{k-1}) = &\prod_{t \in \mathcal{T}_{\text{mis}}(\mathcal{D}_i)} (1 - P_D^t P_G^t p(\chi_k^t \mid \mathbf{Z}^{k-1})) \\ &\times \prod_{t \in \mathcal{T}_{\text{hit}}(\mathcal{D}_i)} (P_D^t P_G^t p(\chi_k^t \mid \mathbf{Z}^{k-1})). \end{aligned} \tag{5}$$

In the next step, consider that $\mathcal{D}_i$ assigns m_1 measurements to track one, m_2 to track two, and m_{n_T} up to track n_T. The total number of combinations for joint association events $\mathcal{H}_{i,j}$ in $\mathcal{D}_i$ is given by the multinominal coefficient. Since all events are a priori equally likely, the a priori probability that event $\mathcal{H}_{i,j}$ is true is given by the inverse of the multinominal:

$$P(\mathcal{H}_{i,j} \mid \mathcal{D}_i, \mathbf{Z}^{k-1}) = \binom{n_k}{n_k - m_T, m_1, \ldots, m_{n_T}}^{-1} = n_M^{-1}, \tag{6}$$

where $m_T = m_1 + \cdots + m_{n_T}$ is the total number of assigned measurements in the detection event $\mathcal{D}_i$.

In the next step, the probability of receiving n_k measurements is defined using the cardinality models $p_c^{Cl}(n)$ for clutter, and $p_c^t(n)$ for the target:

$$p(n_k \mid \mathcal{H}_{i,j}, \mathcal{D}_i, \mathbf{Z}^{k-1}) = p_c^{Cl}(n_k - m_T) \prod_{t \in \mathcal{T}_{\text{hit}}(\mathcal{D}_i)} p_c^t(m_t) \tag{7}$$

In the last step, the probability for the newly received measurement set $\mathbf{Z}_k$, given all the quantities above, is

defined as

$$p(\mathbf{Z}_k \mid n_k, \mathcal{H}_{i,j}, \mathcal{D}_i, \mathbf{Z}^{k-1}) = p_s^{Cl}(n_k - m_T) \prod_{t \in \mathcal{T}_{\text{hit}}(\mathcal{D}_i)} \prod_{l \in \mathcal{M}} p_s^t(\mathbf{z}_k^l \mid \mathbf{x}_k^t). \quad (8)$$

In this equation, $p_s^{Cl}(n)$ is the spatial distribution of clutter and $p(\mathbf{z}_k^l \mid \mathbf{x}_k)$ is the spatial measurement model. The set $\mathcal{M}$ with cardinality m_t comprises of the indices of the measurements assigned to track t in hypothesis $\mathcal{H}_{i,j}$.

Inserting (5), (6), (7) and (8) into (4) finally yields:

$$\begin{aligned} P(\mathcal{H}_{i,j} \mid \mathbf{Z}^k) &= \eta_{\mathcal{H}} \cdot p_s^{Cl}(n_k - m_T) p_c^{Cl}(n_k - m_T) \cdot n_M^{-1} \\ &\times \prod_{t \in \mathcal{T}_{\text{mis}}(\mathcal{D})} (1 - P_G^t P_D^t p(\chi_k^t \mid \mathbf{Z}^{k-1})) \\ &\times \prod_{t \in \mathcal{T}_{\text{hit}}(\mathcal{D})} P_G^t P_D^t p_c^t(m_t) p(\chi_k^t \mid \mathbf{Z}^{k-1}) \prod_{l \in \mathcal{M}} p_s^t(\mathbf{z}_k^l \mid \mathbf{x}_k^t) \end{aligned} \quad (9)$$

Since all feasible association hypotheses are mutually exclusive and form an exhaustive set, the normalization constant $\eta_{\mathcal{H}}$ can be derived by demanding

$$\sum_{\mathcal{H}} P(\mathcal{H}_{i,j} \mid \mathbf{Z}^k) = 1.$$

B. Track-Based Association Probability

From this point, the MD-JIPDA is derived exactly the same way as the JIPDA in [17]: The hypotheses set $\mathcal{H}$ now, in general, contains several hypotheses that assign the same measurement combination for the tth track. Let $\mathcal{A}_i^{m_t}$ denote the ith combination hypothesis of assigning m measurements to a track t with $i = [1, \ldots, \binom{n_k}{m_t}]$. For example from Figure 1, the first two combinations are $\mathcal{A}_1^2 = \{1,4\}$, which assigns detections $M1, M4$ and $\mathcal{A}_2^2 = \{4,7\}$ with detections $M4, M7$.

Let $\tilde{\mathcal{H}} \in \mathcal{H}$ denote the set of hypotheses with a specific combination $\mathcal{A}_i^{m_t}$ assigned to track t. For each combination in $\mathcal{A}_i^{m_t} \setminus \{\mathcal{A}_1^0\}$, the probability that it was generated by t and the object exists, is then given by

$$p(\chi_k^t, \mathcal{A}_i^{m_t} \mid \mathbf{Z}^k) = \sum_{\tilde{\mathcal{H}} \in \mathcal{H}} P(\tilde{\mathcal{H}} \mid \mathbf{Z}^k). \quad (10)$$

The set of hypotheses, where no detection is assigned to a track is denoted $\mathcal{H}^0$. Then, in case of a missed detection, following the probability that the object exists is given by

$$p(\chi_k^t, \mathcal{A}_1^0 \mid \mathbf{Z}^k) = \frac{(1 - P_D^t P_G^t) p(\chi_k^t \mid \mathbf{Z}^{k-1})}{(1 - P_D^t P_G^t p(\chi_k^t \mid \mathbf{Z}^{k-1}))} \sum_{\tilde{\mathcal{H}}^0 \in \mathcal{H}} P(\tilde{\mathcal{H}}^0 \mid \mathbf{Z}^k). \quad (11)$$

The final object existence is given by summing up over all possible measurement combinations $\mathcal{A}_i^{m_t} \in \mathcal{A}$:

$$p(\chi_k^t \mid \mathbf{Z}^k) = \sum_{\mathcal{A}} p(\chi_k^t, \mathcal{A}_i^{m_t} \mid \mathbf{Z}^k) \quad (12)$$

The association likelihoods are then given by

$$p(\mathcal{A}_i^{m_t} \mid \mathbf{Z}^k) = p(\mathcal{A}_i^{m_t} \mid \chi_k^t, \mathbf{Z}^k) = \frac{p(\chi_k^t, \mathcal{A}_i^{m_t} \mid \mathbf{Z}^k)}{p(\chi_k^t \mid \mathbf{Z}^k)}, \quad (13)$$

since assigning a measurement to a track requires the underlying assumption that the track also exists. Since (10)–(13) are basically the same equations as for a point target, the reader is referred to [22, p. 162ff.] for a more detailed derivation.

With the association likelihoods, the new posterior state estimate is computed by

$$p(\mathbf{x}_k^t \mid \mathbf{Z}^k) = \sum_{\mathcal{A}} p(\mathbf{x}_k^t \mid \mathbf{Z}^k, \mathcal{A}_i^{m_t}) p(\mathcal{A}_i^{m_t} \mid \mathbf{Z}^k), \quad (14)$$

where $p(\mathbf{x}_k^t \mid \mathbf{Z}^k, \mathcal{A}_i^{m_t})$ is the computed measurement update for a specific combination e.g. obtained via standard Kalman filtering.

III. IMPLEMENTATION USING RANDOM MATRICES

For the derivation of the MD-JIPDA given above, very few assumptions regarding the sensor model have been made. Since an ET-MOT has to concurrently estimate the object's kinematic state and extension, a large variety for the spatial model $p_s^t(\mathbf{z}_k^{(j)} \mid \mathbf{x}_k^t)$ and measurement cardinality model $p_c^t(m_t)$ are possible. As one possible approach, in this section, the implementation of MD-JIPDA using the Random Matrix framework is briefly described.

It is assumed that each object is of elliptical shape and its extension is described by a symmetric positive definite random matrix $\mathbf{X}_k$. The extension is considered to be statistically independent of the kinematic state and of the cardinality model as well. It shall only influence the spatial model which is then rewritten as $p_s^t(\mathbf{z}_k^{(j)} \mid \mathbf{x}_k^t, \mathbf{X}_k^t)$.

For the measurement cardinality model $p_c^t(m_t)$, using a Poisson distribution is the most common way. However, the expected number of detections per scan can be different for each object. Thus, this parameter, denoted as measurement rate γ_k, has to be estimated in parallel as well.

With these two new quantities, the posterior state estimate is now given by

$$p(\mathbf{x}_k^t, \mathbf{X}_k^t, \gamma_k^t \mid \mathbf{Z}^k) = \sum_{\mathcal{A}} p(\mathbf{x}_k^t, \mathbf{X}_k^t, \gamma_k^t \mid \mathbf{Z}^k, \mathcal{A}_i^{m_t}) p(\mathcal{A}_i^{m_t} \mid \mathbf{Z}^k), \quad (15)$$

The individual steps for solving this equation are explained in the following: First some details on the random matrix framework are given and some considerations on the measurement cardinality model are exemplified. Since for real-time applications, evaluating all possible combinations $\mathcal{A}_i^{m_t}$ may require too much time, in this section, a proposal is made to handle the exponential increase of the hypotheses trees. Finally, the algorithm applied for track birth and deletion is presented as well.

A. Random Matrices

The seminal work for the Random Matrices framework for estimation of extended objects was presented in [4]. Using the Bayes' filter, a concept to estimate kinematic target state and its physical extension in parallel was established. Therefore, the following assumptions on the target characteristics are made: First, it is assumed that the shape of the target can be represented by an ellipse. Further, the direction of the object's motion shall be independent of the orientation of the ellipse.

Finally, as the most important assumption, the noise of the measurements is mainly caused by the physical extension. For a measurement $\mathbf{z}_k^j$ at time k it is assumed that it can be described by a linear function of the state $\mathbf{x}_k$, superimposed by a normally distributed noise term $\mathbf{w}_k$:

$$\mathbf{z}_k^j = \mathbf{H}\mathbf{x}_k + \mathbf{w}_k \tag{16}$$

Assuming that the noise part of the measurement is mainly due to the size of the object, the probability density function for a set of measurements $\mathbf{Z}_k = \{\mathbf{z}_k^1, \ldots, \mathbf{z}_k^{n_k}\}$ is defined as:

$$p(\mathbf{Z}_k \mid n_k, \mathbf{x}_k, \mathbf{X}_k) = \prod_{j=1}^{n_k} \mathcal{N}(\mathbf{z}_k^j; \mathbf{H}\mathbf{x}_k, \mathbf{X}_k) \tag{17}$$

Substituting this relationship in the Bayes' filter recursion leads to an analytic solution for state expectation and covariance update as well as for the update of $\mathbf{X}_k$.

However, for many real-world sensors, the extension driven noise is superimposed by some non-negligible sensor driven measurement noise. For example, radar detections are generally in polar coordinates with range r and detection angle ϕ. Thus, if targets are detected in greater distance, this leads to a larger spread of the measurements in azimuth. Disregarding this fact for the estimation of the physical extension would lead to an overestimation of the true size when the object is far away.

To include the contribution of the sensor error to the measurement spread, [5] proposed the probability density function in the following way:

$$p(\mathbf{Z}_k \mid n_k, \mathbf{x}_k, \mathbf{X}_k) = \prod_{j=1}^{n_k} \mathcal{N}(\mathbf{z}_k^j; \mathbf{H}\mathbf{x}_k, c\mathbf{X}_k + \mathbf{R}_k) \tag{18}$$

However, for this model, no exact analytical solution for $p(\mathbf{x}_k, \mathbf{X}_k \mid \mathbf{Z}^k)$ can be found. To obtain a recursive update scheme, in [5] the assumption is made that the target extent is predicted with sufficient accuracy, which makes it possible to separate kinematic and extension updates.

As already mentioned in the introduction, a more general update scheme using the sensor model as in (18) was presented in [6]. According to [6], this approach has a significant better extension estimate, but at the price of a small decrease in position accuracy, and only if the kinematic state uncertainty is sufficiently small. Some analysis by the authors indicated that in combination with a GPDA, it is also quite vulnerable to false associations. The approach by [5] seems to be more robust, so only this approach is further considered here.

The integration of both update schemes into the GPDA is straight forward: For computation of $p(\mathbf{x}_k, \mathbf{X}_k \mid \mathbf{Z}^k, A_i^m)$ the update schemes can be implemented exactly as given in the cited papers. For the track prediction, the method proposed in [5] is used. For the sake of completeness, the prediction and update equations are given in the appendix.

The final tracker is designed for radar sensors, so for filtering, the detections have to be transformed from polar to Cartesian space using

$$\mathbf{z}_k = \begin{bmatrix} r_k \cos(\phi_k) \\ r_k \sin(\phi_k) \end{bmatrix}. \tag{19}$$

Since the polar measurement standard deviation σ_r for range and σ_ϕ for the detection angle will be small, the associated covariance matrix in Cartesian coordinates is approximated using [24]

$$\mathbf{R}_k \approx \frac{1}{2}(\sigma_r^2 - r_k^2\sigma_\phi^2) \begin{bmatrix} b + \cos(2\phi_k) & \sin(2\phi_k) \\ \sin(2\phi_k) & b - \cos(2\phi_k) \end{bmatrix}$$
$$b = \frac{\sigma_r^2 + r_k^2\sigma_\phi^2}{\sigma_r^2 - r_k^2\sigma_\phi^2}. \tag{20}$$

This makes the measurement noise state dependent, which may have serious impact in the resulting extension estimate.

For the computation of association likelihoods in (9) with the Random Matrix framework, the spatial model is modified to $p_s^t(\mathbf{z}_k^{(j)} \mid \mathbf{x}_k^t, \mathbf{X}_k^t)$. With respect to (18), it is defined to be a normal distribution, with expectation $\mathbf{H}\mathbf{x}_{k|k-1}^t$ and the covariance matrix given by

$$\mathbf{\Sigma}_k = \mathbf{H}\mathbf{P}_{k|k-1}^t\mathbf{H}^T + c\mathbf{X}_{k|k-1}^t + \mathbf{R}_k.$$

B. Cardinality Model

In general, a target is considered to give birth to a random number of detections in each scan. This number is in general Poisson distributed with nearly constant mean γ. In a multi-object scenario, the individual targets may also have different values for γ, which are not known a priori.

As long as the number of detections remains a small single digit value (typ. $\gamma < 5$), it can be sufficient to use an average number over all targets for γ: The Poisson distribution is rather indifferent for those values e.g. for expecting $\gamma = 3$ the measurement probabilities $p_c^t(m)$ for $m = 1 \ldots 6$ are between $[0.05, 0.22]$; if expecting 4, the values are in the same interval. In practice, these little differences have no large impact on the association likelihoods, compared to the spatial models. For example, if m changes, the clutter model with its factor $V^{n_k - m}$ has, in general, an impact factor in the

region to the power of ten, while the cardinality model only changes by a factor of three at most.

However, in the case of higher detection counts, the values of the Poisson distribution differ by orders of magnitude as well. If the expected values are variable, it is necessary to estimate them together with kinematic state and extension. In [13], it was proposed to model the distribution of γ by a Gamma Distribution and estimate its parameters in parallel by assuming that it is actually independent of the kinematic and extension densities. This concept can be applied to the MD-JIPDA as well.

The Gamma p.d.f. is defined with the two parameters $\alpha_k > 0$ and $\beta_k > 0$ as

$$p_{GAM}(\gamma;\alpha_k,\beta_k) = \frac{\beta_k^{\alpha_k}}{\Gamma(\alpha_k)}\gamma^{\alpha_k-1}e^{-\beta_k\gamma}.$$

The expected cardinality is obtained from the expectation value $\gamma_k = \alpha_k/\beta_k$. The cardinality model for the MD-JIPDA is then obtained from the joint likelihood of the Poisson distribution with parameter γ and the gamma distribution using

$$\begin{aligned} p_c^t(m) &= \tilde{\eta}_c \cdot \int p_{POI}(m \mid \gamma) p_{GAM}(\gamma \mid \mathbf{Z}^{k-1}) d\gamma \quad (21)\\ &= \eta_c \cdot \frac{1}{m!}\sum_{\gamma=1}^{n_{\max}} \gamma^{m+\alpha_{k|k-1}^t-1} e^{-\gamma(\beta_{k|k-1}^t+1)}. \end{aligned}$$

The normalization constant η_c has to account for the fact that the constraint $\sum_{m=1}^{n_{\max}} p_c^t(m) = 1$ still must be fulfilled. The computation of the predicted parameters $\alpha_{k|k-1}^t, \beta_{k|k-1}^t$ of the gamma distribution and also its update equations are given in the appendix as well.

C. Hypotheses Generation

It is easy to see that the MD-JIPDA suffers even more from the exponential increase of possible association hypotheses than the standard JIPDA does. To make the MD-JIPDA computationally feasible for complex scenarios with several tracks within one association gate, or if each track can evoke a large number of measurements, an approximation scheme has to be found in such a way that not all theoretically possible combinations have to be evaluated. This reduction problem is a known issue for an ET-MOT. To solve this problem, the RFS approaches, cited in the introduction, use a combination of distance and Expectation Maximization partitioning to cluster nearby measurements and remove unlikely combinations.

For simplification of the MD-JIPDA, a similar concept is proposed in this paper: First, a k-means clustering is applied to the gated measurements for each track individually. The number of clusters should still be larger than the number of tracks in the specific gate. When the number of clusters is chosen too small, the effect that measurements from different objects are put in the same cluster is very likely to happen, as was pointed out in detail in [12]. This would also somehow foil the idea of a PDA since the association tree would be very small. The authors have made good experience if the k-means creates at least as many clusters as three times the number of tracks. This ensures that only very few clusters contain measurements of several objects since each object is sufficiently often split. Of course, dependent on the clutter rate or distribution of the measurements on target, a higher cluster number may be required.

If j clusters have been created, then $C_{\mathcal{A}} \leq 2^j$ single object association combinations are possible. Given n_T tracks in the joint association gate, the total number of joint multi-object hypotheses is $C_{\mathcal{H}} < (C_{\mathcal{A}})^{n_T}$. Even in the case of five clusters per track and three tracks in a common gate, this can lead to several hundred thousand joint hypotheses, which might be beyond of a real-time implementation. Thus, as a second step, it is considered that by the user, a maximum value for $C_{\mathcal{H}}$ is given, from which with the relation above, a maximum value for $C_{\mathcal{A}}$ is derived. Since the number of single object combinations created after the k-means cluster can be significantly higher, from these combinations the $C_{\mathcal{A}}$ best are selected according to the cardinality model (21). Sampling proportional to the cardinality model $p_c^t(m)$ has the advantage that combinations with highly probable detection count m are preferred. For example, if $\gamma = 5$ detections were expected and $C_{\mathcal{A}} = 20$, assuming a pure Poisson distribution, 4 combinations that assign $m = 5$ detections are selected, but only one for $m = 1$. For each count m, the best combinations from the spatial model are chosen. If for a specific count m more combinations are desired than actually available, the next available count is selected. Only for these selected single association combinations, the joint association hypotheses are built. Please note that when using a reduced number of joint hypotheses, the multinominal coefficient in (9) has to be replaced by the actually generated combination count of each joint detection association event.

D. Birth Model

The basis of a new track is formed by those measurements that have not been assigned to a track during the data association process. Based on these detections, first a DBSCAN algorithm is executed to cluster closely spaced measurements. For each cluster, a new track is initialized. The initial existence likelihood is computed based on the number of measurements in a cluster and its distance to existing tracks. Consider a measurement cluster with mean $\bar{\mathbf{z}}$ that contains n_z measurements, then the initial probability is

$$p(\chi_0) = \beta_{\text{birth}} \cdot p_{\text{birth}}^{\text{card}}(n_z) \cdot p_{\text{birth}}^{\text{sp}}(\bar{\mathbf{z}}). \quad (22)$$

The constant β_{birth} denotes the general likelihood, typically selected as the average number of new born objects per scan. The likelihood $p_{\text{birth}}^{\text{card}}(\cdot)$ accounts for the probability that a specific number of detections are part

of a new track. Here, it is proposed to use a typical measurement cardinality model $p_c^{t_{ref}}$ as basis and set

$$p_{\text{birth}}^{\text{card}}(n_z) = \sum_{i=1}^{n_z} p_c^{t_{ref}}(i). \tag{23}$$

This model ensures that if the number of detections in the cluster increases, also the probability of a new track is increased.

The spatial model accounts for the distance between the centroid and already existing tracks:

$$p_{\text{birth}}^{\text{sp}}(\bar{\mathbf{z}}) = 1 - \exp\left(\min_{t\in 1,\ldots,n_T}\{\|\bar{\mathbf{z}} - \mathbf{z}_{k|k}^t\|^2\}/\sigma_d^2\right) \tag{24}$$

The distance $\|\bar{\mathbf{z}} - \mathbf{z}_{k|k}^t\|$ denotes the Euclidean distance between the centroid and the expected measurement of track t. From all available tracks n_T, the minimum distance is selected to evaluate $p_{\text{birth}}^{\text{sp}}$. With the variance σ_d^2, the desired distance from the centroid of an existing track to a new track candidate can be specified.

Each new track is initialized at the center of the selected cluster using the cluster spread as initial extension estimate. If a cluster contains only very few detections, some minimal size should be used to ensure numerical stability. The track is deleted when at any time the existence probability falls below some small threshold.

IV. SIMULATION RESULTS

The performance of multiple detection JIPDA using the Random matrix update schemes given by [5] are evaluated in two sets of Monte Carlo simulations first. One set of simulation is designed with respect to the desired real data application: A high-resolution automotive radar that is mounted on an unmanned surface vessel or a smaller recreational craft. The targets to be tracked are vessels with an overall length below 10 m. For clarity, during maneuvers, in contrast to the true behavior of a vessel, it is assumed that the major axis of the extension ellipse is always aligned with the direction of motion of the object. The second set of simulations is designed to evaluate the capabilities of the MD-JIPDA when a higher number of detections per object is created, and a complete evaluation of the association tree is infeasible.

In all simulations, the coordinated turn model with $\mathbf{x}_k = [x, v_x, y, v_y, \omega]^T$ is used as motion model, with Cartesian positions x, y, the corresponding velocities v_x, v_y and the turn rate ω around the vertical axis.

For the evaluation of each scenario, the modified version of the optimal sub-pattern assignment (OSPA) metric, as introduced in [13], is applied. This modification enhances the OSPA to incorporate also the estimated target size $\mathbf{X}_{k|k}$ and measurement cardinality $\gamma_{k|k}$ of an object.

A. Low Detection Count Scenarios

To evaluate the joint data association, one scenario with four vessels and one scenario with two vessels are considered. For all scenarios, the measurements are assumed to be uniformly distributed over the vessel's extension, and the cardinality is Poisson distributed with constant mean. The sensor reports its measurements in polar coordinates, where the accuracy of a point target is $\sigma_R = 1.0$ m in range and $\sigma_\phi = 0.1^\circ$ for the bearing angle. The observation area is set to 200 m $\times$ 200 m, with the sensor located in the center and its sample time $T = 1/15$ s. Two different clutter rates are considered: A lower case with a mean of 8 false alarms per scan, ($\lambda_8 = 2 \cdot 10^{-4}/\text{m}^2$) and a high clutter case with 80 false positives ($\lambda_{80} = 2 \cdot 10^{-3}/\text{m}^2$). As a further challenge, a different probability of detection is considered in both cases: for the medium case, it is set to 95% and for the high clutter case it is reduced to $p_D = 80\%$.

For tracking and filtering the following parameters are used: The motion model process noise is set to $\sigma_V = 0.1$ m/s^2 and $\sigma_\omega = 1.0^\circ$/s. The sensor noise to extension noise ratio in (18) is set to $c = 1/4$, and the time constant for the capability of changes in the extension is set to 5 s. The decay constant for track existence is set to $\tau_E = 10$ s, and the forgetting factor for target measurement rate parameters $\alpha_{k|k}, \beta_{k|k}$ is set to $\kappa_\gamma = 1.25$ (see prediction step in the appendix).

For the unassigned measurements, the DBSCAN clustering is performed with a distance threshold of 5 m. A new track is created at the cluster's centroid position with an initial existence likelihood of $\beta_{\text{birth}} = 0.01$, a track distance $\sigma_d = 20$ m and a Poisson distribution with a mean of three for $p_c^{t_{ref}}$. The initial position uncertainty is set to $P_0 = \text{diag}\{(3\text{ m})^2, (1/2\text{ m})^2, (3\text{ m})^2, (1\text{ m/s})^2, (1^\circ)^2\}$, and the initial extension is a circle with radius 2 m. If the existence probability falls below the level of 10^{-5}, the track is considered dead, and if the probability exceeds 50%, the track is treated as valid.

The modified OSPA metric uses the cut-off values $c_x = 3$ m, $c_X = 30$ m^2 and $c_\gamma = 2$ with weights $w_x = 0.8$, $w_X = 0.1$ and $w_\gamma = 0.1$. The norm p is just set to one.

1) Scenario A.1: The fist scenario is a typical multi-target scenario to test the general capabilities of the proposed MOT: A total of four different objects are on a straight line trajectory with a nearly constant velocity of about 3 m/s, see Figure 2 and Table I for details. All objects meet at the same area but keep the distance to their centroids mutually of at least four meters. The scenario has a total of 600 samples (40 s). Each object is created and deleted at a different time step. In this scenario, only the suboptimal MD-JIPDA version is applied with limiting the maximum number of joint hypotheses to $1e3$.

The average results for 1000 Monte Carlo Simulation are shown in Figure 3. The tracking cardinality is computed by taking the sum of existence probability over all created tracks at time k: $\sum_t p(\chi_k^t)$. Overall, for both clutter rates and both cardinality models, an acceptable and almost identical performance was achieved. As could be expected, with higher clutter rates and smaller

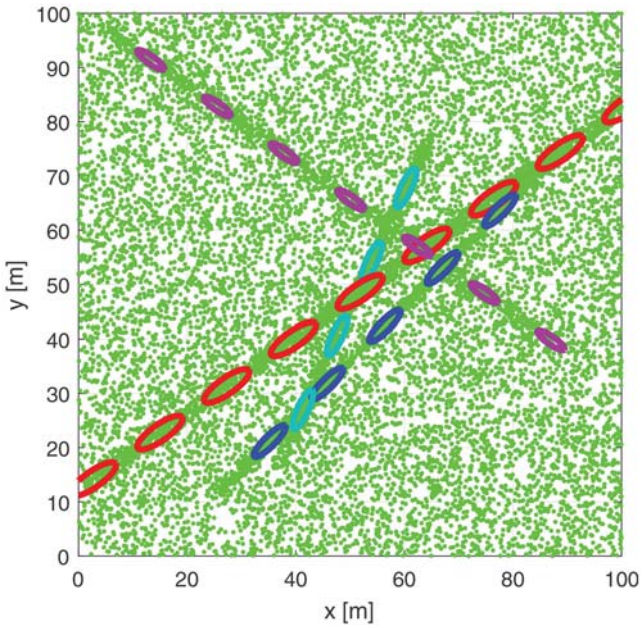

Fig. 2. Targets trajectories and received measurements. Ellipses plotted every five seconds.

TABLE I
Object characteristics for Scenario A. Colors corresponding to Figure 2. The variables A and a denote the length of semi-major and semi-minor axis, respectively.

	Blue	Red	Magenta	Gray
A	4 m	5 m	4 m	3 m
a	1 m	1.5 m	1 m	0.75 m
γ	3	4	3	2
t_{birth}	8 s	0 s	2 s	6 s
t_{death}	34 s	40 s	36 s	28 s

detection probability, the confirmation of a new track takes longer but is still handled fairly well for all objects.

Eye-catching is, of course, the overestimation of objects in case of low clutter with adaptive measurement cardinality. When clutter measurements occur close to a new born target, the measurement data is ambiguous: It could stem from two smaller objects or one large and clutter. However, clutter measurements are in total rare, so the algorithm prefers to keep both tracks alive for a little longer time. Thus, depending on the current distribution of measurements, two tracks moving behind each other are computed as the most likely event. This effect becomes less dominating when the clutter rate increases, since the general track confirmation takes significantly longer. From the OSPA, it is seen that it still actually performs slightly worse than the fixed cardinality model. This is just due to the same effect: Instead of one larger object, two small objects are built. While the fixed model prefers larger objects, and after an initial phase only one object survives, the adaptive cardinality permits two objects, each with an expected cardinality of one or two detections only.

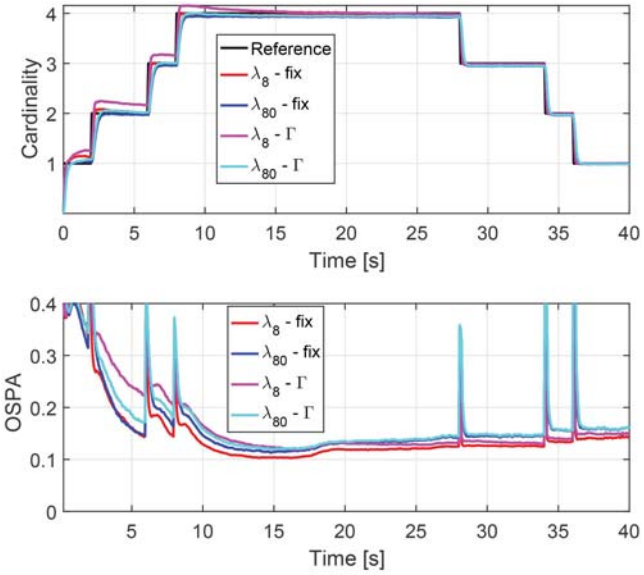

Fig. 3. Track cardinality and OSPA error for different clutter rates. The suffix 'Γ' indicates MD-JIPDA with estimated measurement cardinality, and fix with the constant model.

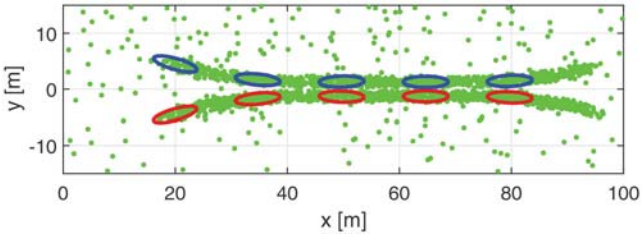

Fig. 4. Trajectories and measurement data for Scenario B. Ellipses plotted every five seconds. The space between both targets is about 22 cm.

2) Scenario B.1: In the second scenario, two objects move towards each other, proceed in parallel for approx. 15 s and then split up again (Figure 4). Both objects have the same characteristics as object 'Blue' from the scenario above. To keep the total number of hypotheses feasible for the MD-JIPDA, a limit of $n_{\max} = 6$ detections per object is set. With this, the scenario enables a comparison between the optimal and its suboptimal version.

The results for 1000 Monte Carlo runs are shown in Figures 5 for the low clutter case, and in 6 for the high clutter case. In these, the additional prefix 'Opt' denotes the results using full MD-JIPDA, 'Sub' denotes the hypothesis limited approach.

Like in the first scenario, an overshoot in the cardinality can be seen when using an adaptive measurement rate Γ. This is again due to the fact that in some runs, two tracks are initialized for one object. Besides this, in all cases, accurate tracks were created for both objects. The fact that the cardinality remains below the true cardinality is due to the limited detection probability P_D. In both OSPA also an increase of the OSPA at about half time can be observed. This is due to another well-known problem of the JIPDA: The track coalescence. Since

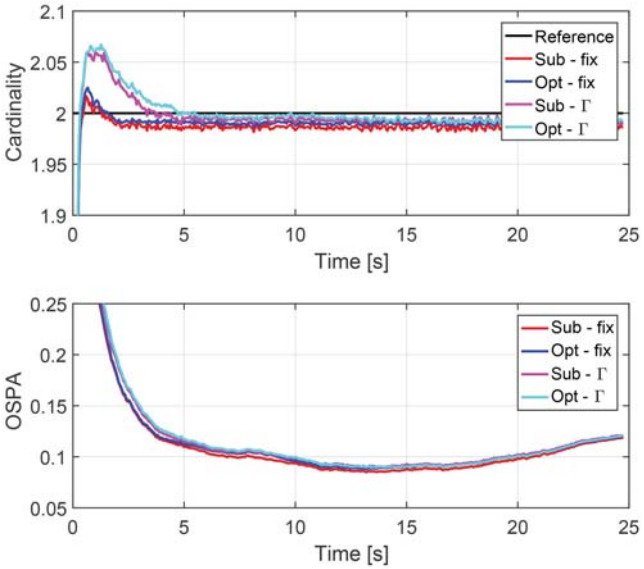

Fig. 5. Track cardinality and OSPA error for medium clutter rate λ_8.

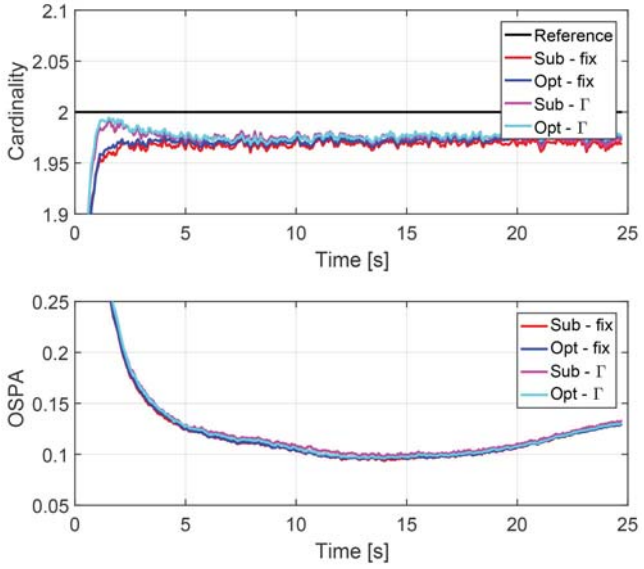

Fig. 6. Track cardinality and OSPA error for high clutter rate λ_{80}.

measurements from the other object are also taken into account, the tracks move closer together. This leads to an overlapping of the extension ellipses in this scenario but with still well-separated target centroids.

These figures also reveal that there is no significant difference between the optimal and the suboptimal approach. Although some slight edge for the optimal approach in cardinality can be seen, it actually also suffers more from track coalescence. Nevertheless, the differences are very small, except for the computation time. These are shown in Table II.[1] In a few runs, over one hour is required to compute the full MD-JIPDA for this scenario. This excluded the algorithm from being used in real-time[2] applications. In contrast, the suboptimal MD-JIPDA with a limited hypotheses count is always within reasonable computation time. Especially with the low clutter scenario, each update step can be handled easily within the update time T. It also has only a small spread between the minimum and maximum required time. The high clutter scenario takes actually more time than the scenario duration. This is due to a large number of tracks that are created and deleted in each update step.

B. High Detection Count

In most cases of the simulations above, the need of clustering or hypotheses limitation for real-time computation is rare. Thus, in this subsection, some of the scenarios above are simulated again using different settings for the measurement model, e.g. an object can create at least 10 detections per step. For this type of sensors, it is even for a single track computationally too expensive to evaluate all possible association hypotheses. However, since e.g. for laser scanner such a measurement count is quite normal, it is important to analyze how the suboptimal approach will perform, and if it can be applied to such problems. Since for this type of sensors the polar sensor noise is low, it is set to zero for these simulations.

TABLE II
Computation Time for the complete sequence of Scenario B.1 for the full MD-JIPDA and the hypothesis reduced suboptimal version. The first value is the mean time over 1000 runs, the value in parentheses the maximum occurred time.

	λ_8 Fix	λ_8 Γ	λ_{80} Fix	λ_{80} Γ
optimal	42 s (4441 s)	33 s (4331 s)	48 s (3278 s)	50 s (1121 s)
suboptimal	13 s (16 s)	13 s (16 s)	37 s (44 s)	40 s (48 s)

1) Scenario A.2: In general, the settings are identical to the previous scenario A.1, except for the target count: Each expected number of measurements in Table I is multiplied with a factor of five, so the expected number is between 10 and 20. In contrast to the scenarios above, with these measurement rates, it is at no time possible to compute a full set of joint association events. The results using the suboptimal with a maximum of 10^4 hypotheses are shown in Figure 7. In these figures, again a comparison with a fixed cardinality model with $\gamma = 15$ and the adaptive scheme are given. As could be expected, only the adaptive scheme handles the scenario correctly, while in the fixed case, for the large red object in many cases, two tracks are established. This effect is again reduced when the clutter rate is higher. For the adaptive scheme, in all runs, the objects are tracked accurately and of course with also better results than in scenario A.1 due to the higher measurement count.

2) Scenario B.2: As a final scenario, the special high clutter scenario as given in [25] is also applied. On the

[1]The values are obtained using single core Matlab simulation on a 3.7 GHz PC.

[2]Here, a tracker is considered real-time applicable when a complete measurement update step can be computed within the sensor's sample time T.

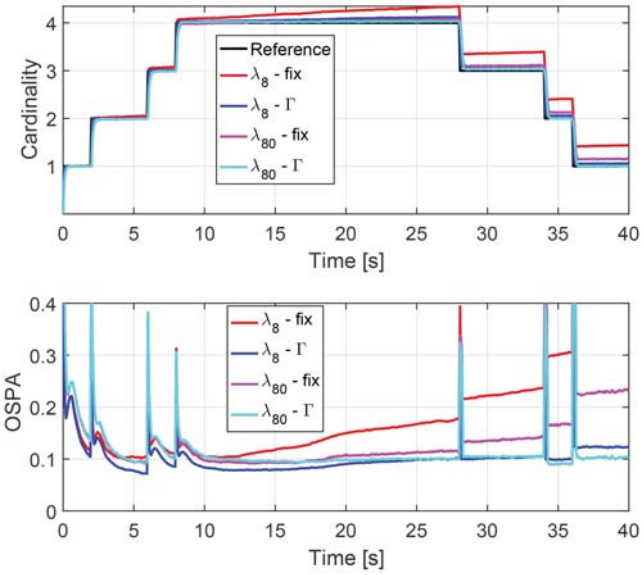

Fig. 7. Track cardinality and OSPA error for different clutter rates for A.2. The suffix 'Γ' indicates MD-JIPDA with estimated measurement cardinality, and 'fix' with the constant model.

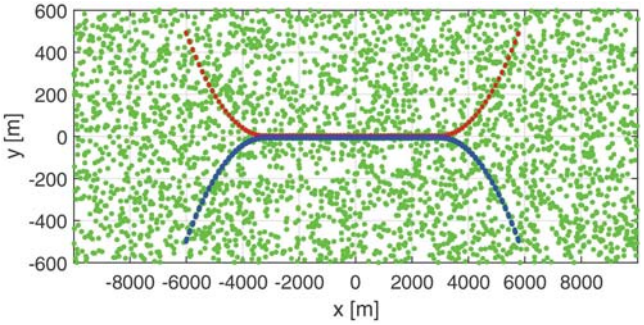

Fig. 8. Target trajectories over the clutter measurement data from *one* scan in the very high clutter case.

first glance, this scenario is similar to the scenario B with a starting turn and a parallel phase (Figure 8). However, the conditions are completely different. Each target is moving with a constant speed of 120 m/s with a distance of less than one meter to the outline of the object during the parallel phase. The first target starts at the south-east, has a size of 40 m × 20 m and generates about $\gamma = 20$ measurements per scan. The second target's dimensions are 20 m × 10 m with an average measurement count of 10.

The parameters for the suboptimal assignment are set to 5 clusters per track and a total maximum of 10^4 hypotheses is chosen.

For this dynamics, the parameters for track initialization and maintenance are therefore changed as follows: The initial position uncertainty is increased to 50 m, and the velocity uncertainty to 80 m/s. The initial extension matrix $\mathbf{X}_0 = 10^2 \times \mathbf{I}_2$ with DOF $\nu_0 = 10$. The cardinality model is initialized with $\alpha_0 = 10$ and $\beta_0 = 1$. The process noise for the velocity is increased to $\sigma_V = 3$ m/s^2. The remaining track parameters and decay constants are the same as in the scenarios above.

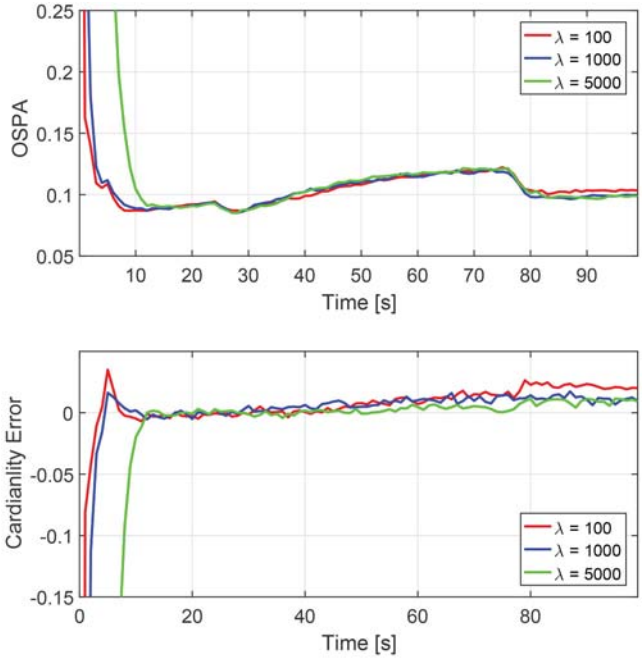

Fig. 9. OSPA and track cardinality error for different clutter rates for scenario B.2.

The scenario is evaluated with three different clutter rates: A low clutter case of 100 false alarms per scan, a high case with 1000 and a very high case with 5000 clutter measurements on a surveillance area of $2 \cdot 10^3$ m × $2 \cdot 10^4$ m. The detection probability is in all cases $p_D = 98\%$.

From Figure 9, it can be seen that the proposed algorithm can handle this type of scenarios also very well. As can be seen, the OSPA error is slowly increasing during the parallel target movement. The problem of track coalescence occurs once more. Due to the measurement clustering by the k-means, this effect is stronger here than in scenario B.1. This also affects the estimated size of the targets, which becomes gradually overestimated, however with a rather slow increase. The issue is resolved, as soon the targets split off again.

V. EXPERIMENTAL RESULTS

For the experimental tests, an automotive radar sensor was mounted on a small vessel. In contrast to the simulation, the radar has an opening angle of only ±26° for a 60 m short range mode and ±9° for larger distances. Due to the limited field of view, the objects under observation are allowed to just perform small maneuvers, as they have to remain inside the field of view (FoV).

The test setup consists of two vessels moving in front of the host vessel (Figure 10). For all three vessels, the GPS traces are recorded. The vessels perform small approaching and bear off maneuvers while slowly

Fig. 10. Target vessels used for data acquisition. The left one (blue) is also used for the single object scenario and has a size of 8.5 m × 2.5 m. The dimensions of the right one (red) are 6.9 m × 2.47 m.

increasing the distance to the host. The recorded trajectory relative to the host and the received measurements are shown in Figure 11.

The tracking algorithm is executed in the body-fixed coordinates of the host vehicle. This requires the compensation of the motion of the host vehicle for each track before performing the update step. Since this is done using the velocity measurement from the GPS and the yaw rate measurement from a low-cost gyro, additional uncertainty is induced into the estimate. To take this into account, for the prediction step, the method proposed by [26] is used to rotate the ellipses according to the motion of the host vessel. However, estimates of the target's yaw rate are not used for extension prediction. The tracking parameters are identical to the values given in the first simulation set for low clutter tracking.

For this scenario, the MD-JIPDA is tested with adaptive measurement rate and a constant rate $\gamma_k = 4$. The cardinality estimates and OSPA results for both schemes are shown in Figure 13, and Figure 12 shows the estimate for the variable approach in a local coordinate frame. From the cardinality plot, it can be seen that in the beginning of the sequence, the fixed γ performs slightly better, but at the end, when the red object moves out of the sensor FoV, it performs significantly worse. This is due to the fact that the target reduces to a point target, which, in combination of a low detection rate, leads to several low estimates of the existence probability. This is compensated by the adaptive version. The OSPA metric is identical for both schemes.

With increasing distance, the number of received detections is decreasing, and so the overshoot, as seen in the simulation, does not occur.

VI. CONCLUSION

This paper presents generalized versions of the JIPDA filter to assign more than one measurement to a

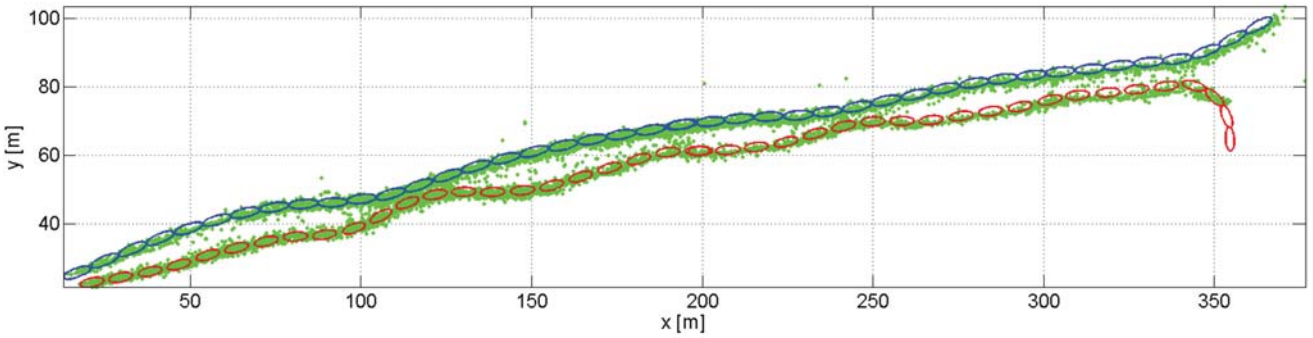

Fig. 11. Reference trajectory of targets (red and blue ellipse) from GPS and received detections (green) in local coordinate frame. The distance to the host vessel during the sequence varies from 20 m to 120 m. The ellipses are plotted in time intervals of 6 s. The scenario starts in the lower left corner, when both ships enter the FoV after overtaking the host vessel. The vessels perform three "draw near and bear away" maneuvers. After about two minutes, the red vessel turns starboard and leaves the FoV (upper right).

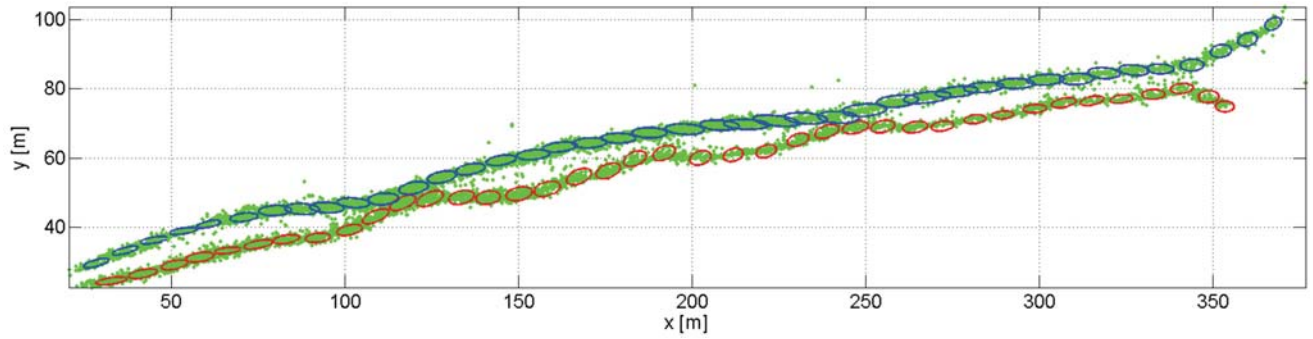

Fig. 12. Estimated trajectory of targets (red and blue ellipse) from MD-JIPDA filter and received detections (green) in local coordinate frame.

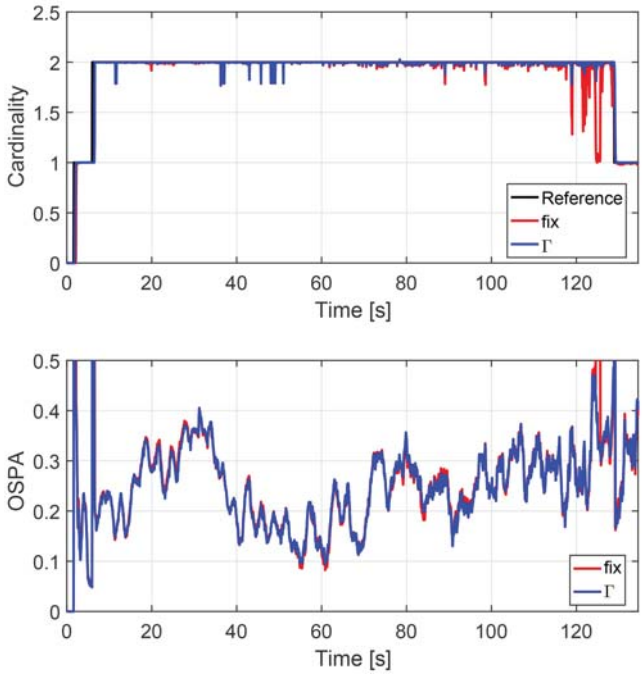

Fig. 13. OSPA metric and number of tracks validated tracks for the experimental data sets.

track. The so-called MD-JIPDA is connected to the random matrix framework to track extended objects with an elliptical shape. To overcome the problem of exponential increase of association hypotheses, a simple cluster and sample technique is applied.

It was shown in simulation and real data scenarios that the proposed MOT algorithm is capable of resolving extended targets, which are moving in close proximity. The results with more complex scenarios indicate that the MD-JIPDA can achieve quite similar results as the RFS approaches. However, like any JPDA, it suffers from track coalescence. Instead, it is the author's opinion, that the MD-JIPDA comes with a reduced complexity e.g. when compared to the recently published LMB. Of course, for a real comparison, the according studies are yet to be made. Another nice feature of the MD-JIPDA is that it can make use of well-known techniques from target tracking, like e.g. gating.

The proposed hypotheses reduction is a rather coarse and intuitive scheme, which offers space for further improvement. An interesting alternative that has to be investigated, is the use of an iterative approach as it was given for the JIPDA in [27]. Starting from the GPDA solution, the association hypothesis tree could be successively expanded up to the desired resolution level. Also, the problem of track coalescence must be addressed by e.g. checking if the techniques from the JPDA can be adopted.

APPENDIX A FILTER STEPS FOR TRACK PREDICTION AND UPDATE

The prediction equations for sample time T are given in Table III and the update equations for track state estimate for an assigned measurement set with n_k detections, centroid $\bar{\mathbf{z}}_k$ and spread $\bar{\mathbf{Z}}_k$ in Table IV.

TABLE III
State filter prediction steps

Kinematic:	$\mathbf{x}_{k\|k-1} = \mathbf{F}_k \mathbf{x}_{k-1\|k-1}$
	$\mathbf{P}_{k\|k-1} = \mathbf{P}_{k-1\|k-1} + \mathbf{F}_k \mathbf{Q}_k \mathbf{F}_k^T$
Extension:	$\mathbf{X}_{k\|k-1} = \mathbf{X}_{k-1\|k-1}$
	$\delta_{k\|k-1} = \delta_{k-1\|k-1} \cdot e^{-T/\tau_\delta}$
Measurement rate:	$\alpha_{k\|k-1} = \frac{1}{\kappa_\gamma} \alpha_{k-1\|k-1}$
	$\beta_{k\|k-1} = \frac{1}{\kappa_\gamma} \beta_{k-1\|k-1}$

TABLE IV
State filter update steps

Kinematic:	$\mathbf{x}_{k\|k} = \mathbf{x}_{k\|k-1} + \mathbf{K}_{k\|k-1}(\bar{\mathbf{z}}_k - \mathbf{H}\mathbf{x}_{k\|k-1})$
	$\mathbf{P}_{k\|k} = \mathbf{P}_{k\|k-1} + \mathbf{K}_{k\|k-1}\mathbf{H}\mathbf{P}_{k\|k-1}^T$
	$\mathbf{S}_{k\|k-1} = \mathbf{H}\mathbf{P}_{k\|k-1}\mathbf{H}^T + \frac{1}{n_k}\mathbf{Y}_{k\|k-1}$
	$\mathbf{K}_{k\|k-1} = \mathbf{P}_{k\|k-1}\mathbf{H}^T\mathbf{S}_{k\|k-1}^{-1}$
	$\mathbf{Y}_{k\|k-1} = c\mathbf{X}_{k-1\|k-1} + \mathbf{R}_k$
Extension:	$\mathbf{X}_{k\|k} = \frac{1}{\delta_{k\|k}}(\delta_{k\|k-1}\mathbf{X}_{k\|k-1} + \hat{\mathbf{N}}_{k\|k-1} + \hat{\mathbf{Y}}_{k\|k-1})$
	$\delta_{k\|k} = \delta_{k\|k-1} + n_k$
	$\mathbf{N}_{k\|k-1} = (\bar{\mathbf{z}}_k - \mathbf{H}\mathbf{x}_{k\|k-1})(\bar{\mathbf{z}}_k - \mathbf{H}\mathbf{x}_{k\|k-1})^T$
	$\hat{\mathbf{N}}_{k\|k-1} = \mathbf{X}_{k\|k-1}^{1/2}\mathbf{S}_{k\|k-1}^{-1/2}\mathbf{N}_{k\|k-1}^{1/2}(\mathbf{S}_{k\|k-1}^{-1/2})^T(\mathbf{X}_{k\|k-1}^{-1/2})^T$
	$\hat{\mathbf{Y}}_{k\|k-1} = \mathbf{X}_{k\|k-1}^{1/2}\mathbf{Y}_{k\|k-1}^{-1/2}\bar{\mathbf{Z}}_k^{1/2}(\mathbf{Y}_{k\|k-1}^{-1/2})^T(\mathbf{X}_{k\|k-1}^{-1/2})^T$
Measurement rate:	$\alpha_{k\|k} = \alpha_{k\|k-1} + n_k$
	$\beta_{k\|k} = \beta_{k\|k-1} + 1$

REFERENCES

[1] M. Blaich, S. Köhler, M. Schuster, J. Reuter, and T. Tietz "Mission integrated collision avoidance for USVs using laser ranger," in *OCEANS 2015 MTS/IEEE*, Genova, 2015.

[2] M. J. Waxman and O. E. Drummond "A bibliography of cluster (group) tracking," *Proc. SPIE*, vol. 5428, pp. 551–560, 2004. [Online]. Available: http://dx.doi.org/10.1117/12.548357.

[3] L. Mihaylova, A. Y. Carmi, F. Septier, A. Gning, S. K. Pang, and S. Godsill
"Overview of Bayesian sequential Monte Carlo methods for group and extended object tracking,"
Digital Signal Processing, vol. 25, no. 0, pp. 1–16, 2014.

[4] J. Koch
"Bayesian approach to extended object and cluster tracking using random matrices,"
Aerospace and Electronic Systems, IEEE Transactions on, vol. 44, no. 3, pp. 1042–1059, 2008.

[5] M. Feldmann, D. Franken, and W. Koch
"Tracking of extended objects and group targets using random matrices,"
Signal Processing, IEEE Transactions on, vol. 59, no. 4, pp. 1409–1420, April 2011.

[6] U. Orguner
"A variational measurement update for extended target tracking with random matrices,"
Signal Processing, IEEE Transactions on, vol. 60, no. 7, pp. 3827–3834, July 2012.

[7] J. Lan and X. Li
"Tracking of extended object or target group using random matrix—Part I: New model and approach,"
in *Information Fusion (FUSION), 2012 15th International Conference on*, July 2012, pp. 2177–2184.

[8] ———
"Tracking of extended object or target group using random matrix—Part II: Irregular object,"
in *Information Fusion (FUSION), 2012 15th International Conference on*, July 2012, pp. 2185–2192.

[9] M. Baum and U. Hanebeck
"Random hypersurface models for extended object tracking,"
in *Signal Processing and Information Technology (ISSPIT), 2009 IEEE International Symposium on*, Dec 2009, pp. 178–183.

[10] M. Wieneke and W. Koch
"A PMHT approach for extended objects and object groups,"
Aerospace and Electronic Systems, IEEE Transactions on, vol. 48, no. 3, pp. 2349–2370, JULY 2012.

[11] M. Wieneke and S. Davey
"Histogram-PMHT for extended targets and target groups in images,"
Aerospace and Electronic Systems, IEEE Transactions on, vol. 50, no. 3, pp. 2199–2217, July 2014.

[12] K. Granström and U. Orguner
"A PHD filter for tracking multiple extended targets using random matrices,"
Signal Processing, IEEE Transactions on, vol. 60, no. 11, pp. 5657–5671, Nov 2012.

[13] C. Lundquist, K. Granström, and U. Orguner
"An extended target CPHD filter and a gamma Gaussian inverse Wishart implementation,"
IEEE Journal of Selected Topics in Signal Processing, vol. 7, no. 3, pp. 472–483, June 2013.

[14] M. Beard, S. Reuter, K. Granström, B. T. Vo, B. N. Vo, and A. Scheel
"Multiple extended target tracking with labeled random finite sets,"
IEEE Transactions on Signal Processing, vol. 64, no. 7, pp. 1638–1653, April 2016.

[15] Y. Bar-Shalom, T. Kirubarajan, and X. Lin
"Probabilistic data association techniques for target tracking with applications to sonar, radar and EO sensors,"
Aerospace and Electronic Systems Magazine, IEEE, vol. 20, no. 8, pp. 37–56, 2005.

[16] D. Musicki, R. Evans, and S. Stankovic
"Integrated probabilistic data association,"
Automatic Control, IEEE Transactions on, vol. 39, no. 6, pp. 1237–1241, 1994.

[17] D. Musicki and R. Evans
"Joint integrated probabilistic data association: JIPDA,"
Aerospace and Electronic Systems, IEEE Transactions on, vol. 40, no. 3, pp. 1093–1099, July 2004.

[18] H. Zhu, T. Ma, S. Chen, and W. Jiang
"A random matrix based method for tracking multiple extended targets,"
in *Information Fusion (FUSION), 2014 17th International Conference on*, July 2014, pp. 1–8.

[19] B. Habtemariam, R. Tharmarasa, T. Kirubarajan, D. Grimmett, and C. Wakayama
"Multiple detection probabilistic data association filter for multistatic target tracking,"
in *Information Fusion (FUSION), 2011 Proceedings of the 14th International Conference on*, July 2011, pp. 1–6.

[20] B. Habtemariam, R. Tharmarasa, T. Thayaparan, M. Mallick, and T. Kirubarajan
"A multiple-detection joint probabilistic data association filter,"
Selected Topics in Signal Processing, IEEE Journal of, vol. 7, no. 3, pp. 461–471, June 2013.

[21] R. Schubert, C. Adam, E. Richter, S. Bauer, H. Lietz, and G. Wanielik
"Generalized probabilistic data association for vehicle tracking under clutter,"
in *Intelligent Vehicles Symposium (IV), 2012 IEEE*, 2012, pp. 962–968.

[22] S. Challa, M. R. Morelande, D. Musicki, and R. J. Evans
Fundamentals of Object Tracking.
Cambridge University Press, 2011, cambridge Books Online. [Online]. Available: http://dx.doi.org/10.1017/CBO9780511975837.

[23] R. P. Samuel Blackman
Design and Analysis of Modern Tracking Systems.
Artech House Boston, 1999.

[24] D. Lerro and Y. Bar-Shalom
"Tracking with debiased consistent converted measurements versus EKF,"
Aerospace and Electronic Systems, IEEE Transactions on, vol. 29, no. 3, pp. 1015–1022, Jul 1993.

[25] S. Reuter, M. Beardy, K. Granström, and K. Dietmayer
"Tracking extended targets in high clutter using a GGIW-LMB filter,"
in *Sensor Data Fusion: Trends, Solutions, Applications (SDF), 2015*, Oct 2015, pp. 1–6.

[26] K. Granström and U. Orguner
"New prediction for extended targets with random matrices,"
IEEE Transactions on Aerospace and Electronic Systems, vol. 50, no. 2, pp. 1577–1589, 2014.

[27] T. L. Song, H. W. Kim, and D. Musicki
"Iterative joint integrated probabilistic data association for multitarget tracking,"
Aerospace and Electronic Systems, IEEE Transactions on, vol. 51, no. 1, pp. 642–653, January 2015.

Michael Schuster received his master degree in electrical engineering in 2010 from the Konstanz University of Applied Science. He is working as research assistant towards his Ph.D. at Chemnitz University of Technology in cooperation with Konstanz University of Applied Sciences. His research interests include data fusion, target tracking, and advanced driver assistance systems.

Johannes Reuter received Dipl. Ing. and Ph.D. degrees in 1995 and 2000, both from Technische Universität Berlin. From 2000 to 2001 he worked as a development engineer for IAV GmbH Berlin and from 2001 to 2004 as a development engineer and department manager for IAV Automotive Engineering Inc. in Ann Arbor MI, USA. From 2004 to 2007 he was with the Innovation Center of EATON Corporation in Southfield MI, USA. Since 2007 he has been a Professor for Automatic Control Systems at University of Applied Sciences Konstanz. His current research interests are related to multi sensor data fusion, autonomous maritime systems, observer-based control of magnetic actuators and renewable energy systems.

Gerd Wanielik received his Ph.D. in 1988 from the Technical University of Karlsruhe (Germany) in electrical engineering. From 1979 he has worked as a scientist at the AEG-Telefunken Research Institute and later at the Daimler Chrysler Research Center. Since 1999 he has been Professor of Communication Engineering at the Chemnitz University of Technology (Germany). His research interests include multi sensor processing and systems, polarimetry, communication and navigation systems.